Physics-informed machine learning for prediction of sea ice dynamics derived from spaceborne passive microwave data

1st Younghyun Koo
Department of Computer Science & Engineering
Department of Civil & Environmental Engineering
Lehigh University
Bethlehem, PA, USA
yok223@lehigh.edu

2nd Maryam Rahnemoonfar
Department of Computer Science & Engineering
Department of Civil & Environmental Engineering
Lehigh University
Bethlehem, PA, USA
mar822@lehigh.edu

2024 IEEE Radar Conference (RadarConf24) | 979-8-3503-2920-9/24/$31.00 ©2024 IEEE | DOI: 10.1109/RADARCONF2458775.2024.10549268

***Abstract*—Spaceborne passive microwave (PMW) images have been used as primary data sources to obtain sea ice concentration (SIC) and sea ice velocity (SIV) information in the polar oceans. Based on the PMW satellite observations and meteorological air temperature and wind data, we develop a fully convolutional neural network to predict daily SIC and SIV. When training this deep learning model, instead of using a fully data-driven approach, we integrate physical knowledge about sea ice dynamics to regulate the prediction results into physically valid values. This physics-informed learning is conducted by including the physics loss function that is independent of the data loss function. Our experiment shows that the physics loss function improves SIC and SIV predictions for most of the Arctic Ocean and winter seasons. The enhancement by the physics loss function appears more substantial when we predict SIV with a small number of training samples.**

***Index Terms*—Physics-informed machine learning, passive microwave, sea ice, sea ice concentration, sea ice drift**

I. Introduction

According to various satellite observations, the Arctic sea ice extent and thickness have dramatically decreased over the last few decades. Sea ice extent has been reduced by more than 50,000 km^2/year because of anthropogenic CO2 emission and global warming [1]. At the same time, the Arctic sea ice thickness has decreased by more than 2 m, leading to the loss of thick multi-year ice by more than 50 % [2]. Along with such dramatic changes in sea ice extent and thickness, the thermodynamic and dynamic conditions of the Arctic sea ice have encountered a new phase [3], [4]. In particular, since the dynamic movement of sea ice is highly correlated to sea ice area and sea ice volume, it is essential to understand both sea ice dynamics and area fraction as a clue in the future of the Arctic Ocean and global climate.

A main tool to monitor global sea ice dynamics in polar regions is satellite passive microwave (PMW) images. Multichannel passive microwave images have primarily provided daily or bi-daily estimates of sea ice concentration (SIC) over the polar oceans since 1978 [5]. The SIC retrieval algorithms of PMW are based on the assumption that the variations in brightness temperature result from the spatial variations in SIC change and ice temperature [6], [7]. These algorithms have used the empirical linear relationship between SIC and brightness temperature from multiple PMW frequencies and polarizations. In addition, PMW images have been used to retrieve sea ice velocity (SIV) by tracking structures in sea ice cover in a pair of consecutive PMW images [8]. Although the spatial resolutions of the PMW-based sea ice observations (tens-of-km scale) are not as fine as optical images (tens-of-meters scale), PMW images have been the most effective way for sea ice monitoring because of their penetrability over clouds and daily global coverage.

Hence, by assimilating these spaceborne PMW-based sea ice observations and physical knowledge of sea ice dynamics, many numerical sea ice models have been developed and calibrated to predict the Arctic sea ice motions [9], [10]. These sea ice models rely on a physical understanding of sea ice and its interaction with the atmosphere and ocean. However, such physics models require too many complicated parameterizations accompanying high computational costs to run the models. Moreover, considering that numerical models are highly sensitive to initial conditions and physical assumptions, their results can be inconsistent with real observations [11].

Recently, machine learning (ML) techniques, particularly deep learning, have emerged as alternatives for physics numerical models to forecast sea ice conditions, including both SIC and SIV. Various deep learning models, including convolutional neural networks (CNN) and recurrent neural networks (RNN), have been used to predict daily SIC from PMW data [12]–[14]. Besides SIC, CNN and RNN have also been used to predict daily SIV, outperforming other statistical methods [15], [16].

However, since sea ice movement is extremely complicated due to the interaction between the atmosphere and ocean, a fully data-driven machine learning approach can introduce significant uncertainties in the prediction result. In particular, if the number of training datasets is not enough or the training datasets contain significant noises, the fidelity of the fully data-

driven models can deteriorate. Moreover, the physical variables predicted by such a fully data-driven approach can sometimes be physically inconsistent or implausible [17]. Therefore, it is necessary to integrate fundamental physical laws and domain knowledge into the ML training as informative priors. By including prior knowledge or constraints, the ML model can yield more interpretable predictions even in the presence of imperfect data, such as missing, noise, or outliers data [17].

Thus, this study develops a fully convolutional deep learning model performing daily forecasting of SIC and SIV, and we aim to improve the model fidelity by integrating the physical knowledge in the model training. In order to guarantee valid SIC and SIV values in the prediction, we add a physics loss term that reflects the physical relationship between SIC and SIV. The main contributions of this research work consist of the following.

- We propose a physics loss function to integrate intrinsic sea ice dynamics into deep learning training and regulate the valid sea ice concentration and velocity range.
- The proposed physics loss function is added to a multi-task fully convolutional network to predict daily sea ice concentration and velocity.
- Our extensive experiments show that the physics loss function improves accuracy in SIC and SIV predictions, even when the number of training samples is insufficient.

II. Related work

A. Physics in sea ice dynamics

It is known that dynamic and thermodynamic mechanisms determine the spatiotemporal changes in SIC. The evolution of SIC (A) is expressed by the following equation [18]:

$$\frac{\partial A}{\partial t} + \nabla \cdot (\boldsymbol{u} A) = f_c - r \tag{1}$$

where $\boldsymbol{u}$ is ice motion, f_c is the ice concentration change from freezing or melting (thermodynamic mechanisms), and r is the concentration change from mass-conserving mechanical ice redistribution processes (e.g., ridging or rafting) that convert ice area to ice thickness.

Additionally, numerous physical sea ice models have proposed the following mathematical equation to explain sea ice dynamics by assuming the elastic-viscous-plastic (EVP) properties of sea ice [19]:

$$m\frac{D\boldsymbol{u}}{Dt} = -mf\boldsymbol{k} \times \boldsymbol{u} + \tau_{ai} + \tau_{wi} + \boldsymbol{F} - mg\nabla H \tag{2}$$

where $D/Dt = \partial/\partial t + \boldsymbol{u} \cdot \nabla$ is the substantial time derivative, m is the ice mass per unite area, $\boldsymbol{k}$ is a unit vector normal to the surface, $\boldsymbol{u}$ is the ice velocity, f is the Coriolis parameter, τ_{ai} and τ_{wi} are the forces due to air and water stresses, H is the elevation of the sea surface, g is the gravity acceleration, and $\boldsymbol{F}$ is the force due to variations in internal ice stress. As many previous studies have already suggested, wind and ocean forcings have primary impacts on SIV and dynamics. Particularly, wind velocity has been treated as a major variable in SIV, which can contribute to up to 70 % of the sea ice velocity variances [20] depending on season or region. Nevertheless, predicting sea ice dynamics based on physical models is still challenging due to its intrinsic complexity and dependency on numerous atmospheric and oceanic parameterizations.

B. Neural network for sea ice prediction

Convolutional neural networks (CNN) are the most popular and efficient deep learning network to predict SIC and SIV. First, regarding SIC, Andersson et al. [21] proposed a deep-learning sea ice forecasting system named IceNet, designed to forecast monthly sea ice concentration for the next six months. Kim et al. [22] used CNN to predict after-one-month SIC from satellite-based SIC observations and weather data for the previous months, and their model showed a mean absolute error (MAE) of 2.28% and correlation coefficient of 0.98. Similarly, a CNN model proposed by Ren et al. [12] showed < 1 % of MAE in daily SIC prediction for melting season, and U-Net by Ren et al. [23] showed 2-3 % of MAE in daily SIC prediction. When it comes to SIV, a CNN model proposed by Hoffman et al. [15] showed approximately 0.8 correlation coefficient in SIV prediction. Additionally, Koo et al. [24] proposed a multi-task CNN to predict daily SIC and SIV simultaneously. However, to our knowledge, no studies have attempted to integrate physics knowledge embedded in sea ice dynamics into CNN or any other neural networks. Therefore, this study is the first to apply a physics-informed neural network for sea ice prediction.

III. Data

We collect SIC and SIV satellite observation data retrieved from PMW sensors of the NOAA (National Oceanic and Atmospheric Administration) satellites as the primary input of the models (Fig 1). We also collect wind and air temperature data from the ERA5 climate reanalysis product as additional input variables.

A. Sea ice concentration

SIC satellite observation is from NOAA/NSIDC Climate Data Record of Passive Microwave Sea Ice Concentration version 4 data [25]. This data provides a Climate Data Record (CDR) of SIC (i.e., the areal fraction of sea ice within a grid cell) from PMW sensors, such as Special Sensor Microwave Imager (SSMI) and Special Sensor Microwave Imager/Sounder (SSMI/S) (Table I). The CDR algorithm output is the combination of SIC estimations from two algorithms: the NASA Team (NT) algorithm and NASA Bootstrap (BT) algorithm. These empirical algorithms estimate SIC from the PMW brightness temperatures at different frequencies and polarizations (i.e., vertical and horizontal polarizations at 19 GHz, 22 GHz, and 37 GHz). Then, this CDR product adjusts algorithm coefficients for each sensor to optimize the consistency of daily and monthly SIC time series.

B. Sea ice drift

SIV data are acquired from the NSIDC Polar Pathfinder Daily 25 km EASE-Grid Sea Ice Motion Vectors version 4

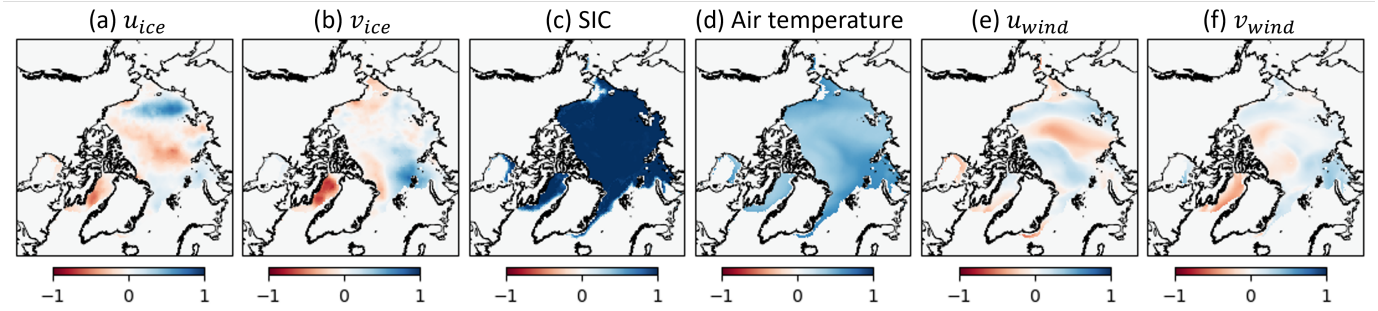

Fig. 1. Normalized 6 input variables: (a) u-component sea ice velocity, (b) v-component sea ice velocity, (c) sea ice concentration, (d) air temperature, (e) u-component wind velocity, and (f) v-component wind velocity. Sea ice velocity and concentration are acquired from multiple passive microwave sensors, and air temperate and wind velocity are acquired from the ERA5 climate reanalysis. This snapshot is from January 1st, 2022.

TABLE I
KEY PARAMETERS OF PASSIVE MICROWAVE IMAGES USED TO RETRIEVE SEA ICE CONCENTRATION AND SEA ICE DRIFT DATASETS

PMW Sensor	**Frequency (GHz)**	**Footprint (km)**	**Spacing (km)**
Special Sensor Microwave Imager (SSM/I)	19V/19H 22V 37V/37H	69×43 60×40 37×28	25×25 25×25 25×25
Special Sensor Microwave Imager / Sounder (SSMIS)	19V/19H 22V 37V/37H	72×44 72×44 44×26	45×74 45×74 28×45
Advanced Microwave Scanning Radiometer (AMSR-E)	89V	6×4	5×5

[26]. This product derives daily sea ice drift from three primary types of sources: (1) gridded satellite imagery (e.g., Advanced Very High-Resolution Radiometer (AVHRR), SMMR, SSMI, SSMI/S, Advanced Microwave Scanning Radiometer (AMSR)) (Table I), (2) wind reanalysis data, and (3) buoy position data from the International Arctic Buoy Program (IABP). The u component (along-x) and v component (along-y) of sea ice motions are independently derived from these sources and optimally interpolated onto a 25 km EASE grid by combining all sources. After a correlation coefficient is calculated between a small target area in one image and a searching area in the second image, the location in the second image where the correlation coefficient is the highest is determined as the displacement of ice [26].

C. ERA5 climate reanalysis

Wind and air temperature can have significant impacts on sea ice motion and thermodynamic freezing and melting of sea ice. Thus, we use wind velocity and air temperature from ERA5 climate reanalysis as the input of our neural network models. ERA5 is the fifth generation ECMWF (European Centre for Medium-Range Weather Forecasts) atmospheric reanalysis of the global climate covering the period from January 1940 to the present [27]. We acquire the daily average wind velocity (u and v components) at 10 m height and 2 m air temperature. The raw ERA5 gridded data of 0.25 degrees are projected onto the 25 km EASE grid using bilinear interpolation to co-locate with the sea ice drift data.

IV. METHOD

Generally, the most common ways to embed prior physics knowledge in neural networks are (1) introducing appropriate loss functions that satisfy physical constraints or (2) designing network architectures that guarantee physical constraints [17]. In this study, to embed fundamental knowledge of sea ice dynamics, we introduce physics loss functions in the training phase of an existing convolutional network architecture. This section presents what neural network architecture and loss functions are used in this study.

A. Hierarchical information-sharing U-net

The Hierarchical information-sharing U-net (HIS-Unet) (Fig 2) [24] is used as a deep learning model to predict SIC and SIV. HIS-Unet consists of two separate SIC and SIV branches of U-net-shaped fully convolutional networks, which share the first convolutional layer. The kernel size of the convolutional layer is set to 3×3, and the hyperbolic tangent (tanh) activation function is applied after each convolution. These SIC and SIV branches share and highlight their information through weighting attention modules (WAMs). Since these WAMs contain linear weighting parameters and channel/spatial attention modules, the SIC and SIV information is mixed up with their relative importance, and more important information is highlighted in WAMs. This HIS-Unet architecture shows a better performance than other fully convolutional networks and statistical approaches in the daily prediction of SIC and SIV in the Arctic Ocean [24]. In particular, HIS-Unet is more successful than other models in (1) the late melting season and early freezing season and (2) marginal sea ice zones near coastal regions out of the central Arctic [24].

B. Physics loss function

Based on the HIS-Unet model, we modify the loss function to consider physical constraints. Our objective loss function consists of (1) a data loss term represented by mean square error (MSE) and (2) a physics loss term inspired by physical constraints.

First, the MSE data loss term (L_D) can be calculated by the following equation with u-component SIV (u), v-component SIV (v), and SIC (A):

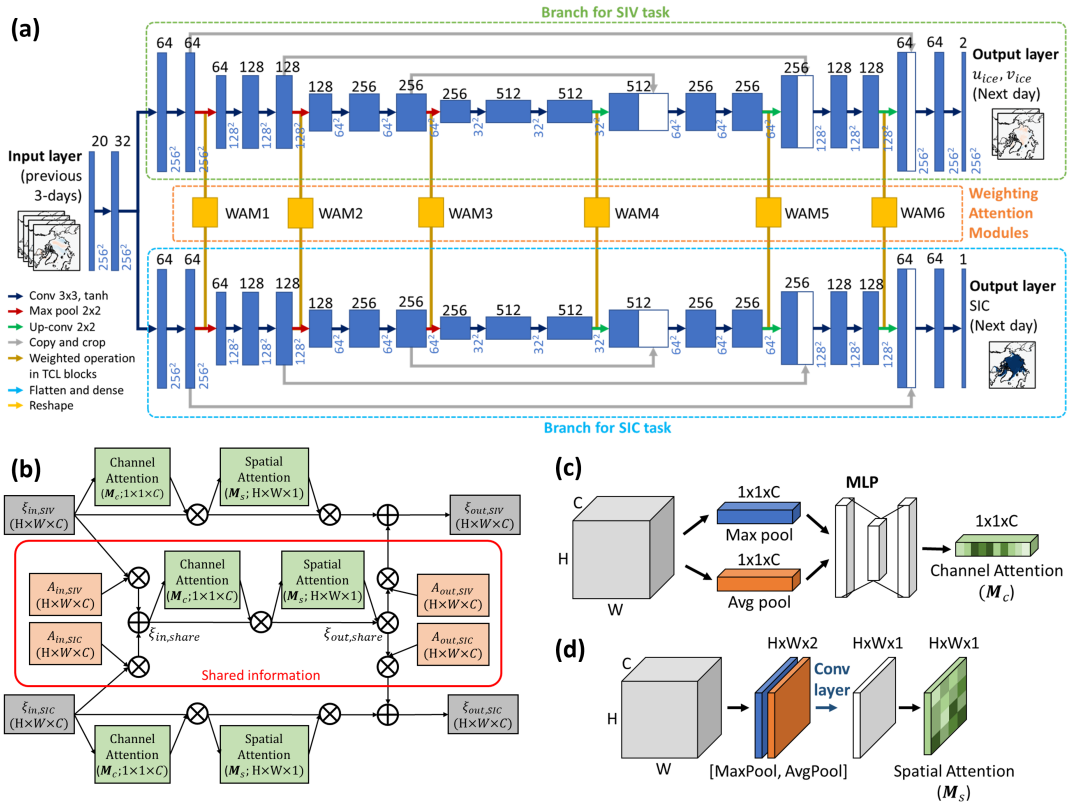

Fig. 2. (a) Architecture of Hierarchical information-sharing U-net (HIS-Unet); (b) Weighting attention module (WAM) in HIS-Unet; (c) channel attention module and (d) spatial attention module in WAM [24]

$$L_{data} = \sum(|u_p - u_o|^2 + |v_p - v_o|^2 + |A_p - A_o|^2) \quad (3)$$

where the subscript o means observation (ground-truth) and p means prediction by HIS-Unet.

Next, we propose a first physics loss term (L_{phy1}) based on the valid SIC values. Since the valid SIC values range from 0 to 1 (i.e., 0-100 %), we add a penalty if the predicted SIC value exceeds this valid range as follows:

$$L_{phy1} = \sum(|min(0, A_p)| + |max(0, A_p - 1)|) \quad (4)$$

The second physics loss term (L_{phy2}) represents the valid SIV values associated with SIC values. Since the SIV data we use defines valid sea ice motion only where SIC is greater than 15 % [26], the SIV value should be zero where SIC is less than 15 %. Therefore, we define the second physics loss term as follows:

$$L_{phy2} = \begin{cases} |u_p^2 + v_p^2|, & \text{if } A_p < 0.15 \\ 0, & \text{if } A_p \geq 0.15 \end{cases} \quad (5)$$

The last physics loss term (L_{phy3}) is based on Eq. 1, which explains the thermodynamic and dynamic SIC changes. As shown in Eq. 1, the thermodynamic SIC changes (f_c) and mechanical ice redistribution (r) can be calculated by temporal changes of SIC and the combination of advection and divergence of SIC. Since we focus on daily SIC prediction, the daily variations of the right term in Eq. 1 (i.e., $f_c + r$) should not exceed (-1, 1). We assume that the combination of thermodynamic SIC changes and mechanical ice redistribution cannot saturate SIC from 0 % to 100 % or remove the entire sea ice from 100 % to 0 % within a day. Based on this assumption, we propose the following physics loss term:

$$L_{phy3} = \text{ReLU}(|\frac{\partial A_p}{\partial t} + \nabla \cdot (\boldsymbol{u}_p A_p)| - 1) \quad (6)$$

where the time derivative term ($\frac{\partial A_p}{\partial t}$) is derived by subtracting the previous-day SIC from the output SIC, and the spatial derivative term ($\nabla \cdot (\boldsymbol{u}_p A_p)$) is derived from the gradients in output SIV and SIC grids.

Consequently, the total physics loss term (L_{phy}) and the final objective loss functions (L) are defined as follows:

$$L_{phy} = L_{phy1} + L_{phy2} + L_{phy3} \quad (7)$$

$$L = L_{data} + \lambda L_{phy} \quad (8)$$

where λ is the weight for the physics loss term, which is set to 1.0 in this study.

C. Experiment setup

As the input of the model to predict the daily SIV and SIC, we use the previous 3-days of SIV (u- and v- compo-

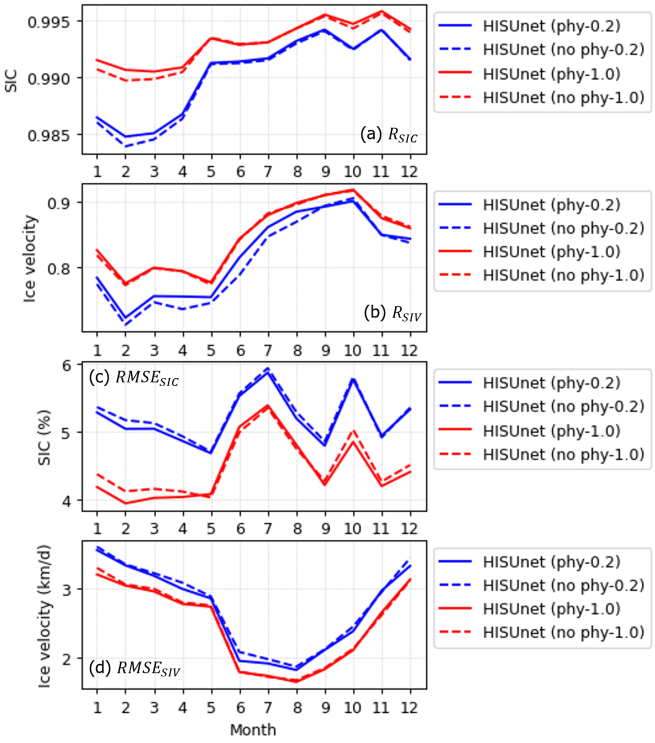

Fig. 3. Comparison of monthly accuracy of the models: (a) R of SIC, (b) R of SIV, (c) RMSE of SIC, and (d) RMSE of SIV

nents), SIC, air temperature, and wind velocity (u- and v-components). Consequently, the input layer has 18 channels of 256×256 grid size. All input values are normalized to -1 to 1 based on the nominal maximum and minimum values that each variable can have. We collect the data from 2016 to 2022; 2016-2021 datasets are used to train/validate the model, and 2022 datasets are used to test the model. To check how the physics loss function improves the model fidelity in small data samples, we train the model with two different training sample sizes: (1) using all 2016-2021 data as training samples (i.e., 100 % sampling) and (2) randomly selecting 20 % of 2016-2021 data as training samples (i.e., 20 % sampling). The total number of training samples is 2177 and 436 for the 100 % sampling and the 20 % sampling, respectively. We assess and compare the results from the HIS-Unet with those two different training sample cases and with or without physics loss function. The loss functions are optimized by Adam stochastic gradient descent algorithm with 100 epochs and 0.001 learning rate. All scripts are executed on eight NVIDIA RTX A5000 GPUs with 24 GB memory.

V. Results

Table II shows the accuracy of SIC for HIS-Unet with and without physics loss function using 20 % and 100 % training samples. Since 100 % sampling allows more samples during the model training, it is reasonable that 100 % sampling always shows a better accuracy than 20 % sampling. It is also noted that the inclusion of the physics loss function slightly

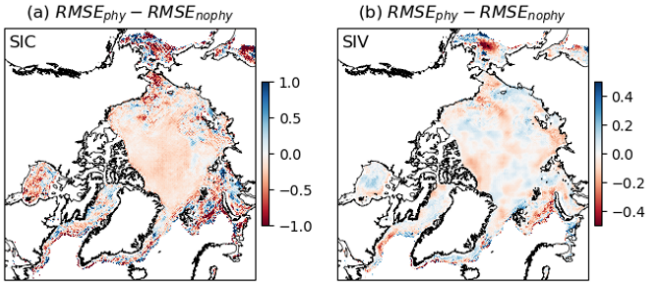

Fig. 4. (a) The difference of sea ice concentration RMSE between HIS-Unet with physics loss function and without physics loss function; (b) The difference of sea ice velocity RMSE between HIS-Unet with physics loss function and without physics loss function

TABLE II
Accuracy of Sea Ice Concentration for Different Training Samples and Neural Network Models

Training samples	Model	R	RMSE (%)
20 %	w/ L_{phy}	**0.990**	**5.197**
	w/o L_{phy}	0.990	5.253
100 %	w/ L_{phy}	**0.993**	**4.437**
	w/o L_{phy}	0.992	4.500

improves the SIC accuracy for both training samples: root mean square error (RMSE) reduces by 0.056 % for 20 % samples and 0.063 % for 100 % samples. When it comes to monthly comparison (Fig 3a and 3c), the physics loss function contributes to improving SIC prediction, particularly in winter months from January to April. Furthermore, as shown in Fig 4a improvements in SIC prediction are observed in most of the Arctic Ocean, particularly near the Bering Sea and Barents Sea, where the RMSE of SIC decreases by up to 1 % by adopting the physics loss function.

Next, table III shows the accuracy of SIV for the same models and the same sampling cases. Similar to the SIC cases, 100 % sampling shows better accuracy than 20 % sampling, and the models trained with the physics loss function show better accuracy. RMSE of the with-physics model is less than the without-physics model by 0.053 km/day for 20 % samples and 0.016 km/day for 100 % samples. While the improvement of SIC prediction by physics loss term does not vary much with the number of training samples (Table II), the improvement of SIV prediction by the physics loss function is more significant for fewer training samples. The physics loss function contributes to the SIV prediction consistently over the season (Fig 3b and d) and evenly over the Arctic Ocean

TABLE III
Accuracy of Sea Ice Velocity for Different Training Samples and Neural Network Models

Training samples	Model	R	RMSE (km/day)
20 %	w/ L_{phy}	**0.818**	**2.699**
	w/o L_{phy}	0.808	2.752
100 %	w/ L_{phy}	**0.846**	**2.468**
	w/o L_{phy}	0.845	2.484

(Fig 4b). However, some regions near the East Siberian and Beaufort Seas do not show improvements in SIV prediction with the physics-loss function.

VI. Conclusion

This study uses the sea ice datasets from passive microwave (PMW) satellite images and a deep learning model to predict daily sea ice concentration (SIC) and sea ice velocity (SIV). We obtain more accurate and physically plausible prediction results by employing a physics loss function in addition to a fully data-driven mean square error loss function. Extensive experiments are implemented using the Hierarchical information-sharing U-net (HIS-Unet) and sea ice datasets derived from PMW images from 2016 to 2022. In order to investigate the impact of training samples on the model robustness, the models are trained with two different training samples: (i) all available training samples (100 %) and (ii) 20 % of training samples. The results exhibit that the physics loss function slightly improves the SIC and SIV predictions. The improvement of SIC prediction is more significant in winter seasons from January to April and for the entire Arctic Ocean; meanwhile, the SIV improvement is also observed over the Arctic Ocean and throughout the year. While the SIV improvement is not so significant when the model is trained with all training samples, it becomes more significant when only 20 % of the total samples are used for training. This result implies that the integration of physics knowledge into deep learning can contribute to the accurate forecast of sea ice dynamics, even in case of a lack of sufficient datasets.

Acknowledgment

This work is supported by NSF BIGDATA (IIS-1838230, 2308649) and NSF Leadership Class Computing (OAC-2139536) awards.

References

[1] D. Notz and J. Stroeve, "Observed arctic sea-ice loss directly follows anthropogenic CO2 emission," Science, vol. 354, no. 6313, pp. 747–750, 2016.

[2] R. Kwok, "Arctic sea ice thickness, volume, and multiyear ice coverage: losses and coupled variability (1958–2018)," Environmental Research Letters, vol. 13, p. 105005, Oct 2018.

[3] R. Kwok, G. Spreen, and S. Pang, "Arctic sea ice circulation and drift speed: Decadal trends and ocean currents," Journal of Geophysical Research: Oceans, vol. 118, no. 5, pp. 2408–2425, 2013.

[4] J. Anheuser, Y. Liu, and J. R. Key, "A climatology of thermodynamic vs. dynamic arctic wintertime sea ice thickness effects during the cryosat-2 era," The Cryosphere, vol. 17, no. 7, pp. 2871–2889, 2023.

[5] W. N. Meier, G. Peng, D. J. Scott, and M. H. Savoie, "Verification of a new NOAA/NSIDC passive microwave sea-ice concentration climate record", POLAR, vol. 33, Dec. 2014.

[6] D. J. Cavalieri, P. Gloersen, and W. J. Campbell, "Determination of sea ice parameters with the nimbus 7 smmr," Journal of Geophysical Research: Atmospheres, vol. 89, no. D4, pp. 5355–5369, 1984.

[7] J. C. Comiso, "Characteristics of arctic winter sea ice from satellite multispectral microwave observations," Journal of Geophysical Research: Oceans, vol. 91, no. C1, pp. 975–994, 1986.

[8] S. Sandven, G. Spreen, G. Heygster, F. Girard-Ardhuin, S. L. Farrell, W. Dierking, and R. A. Allard, "Sea Ice Remote Sensing—Recent Developments in Methods and Climate Data Sets," Surveys in Geophysics, vol. 44, pp. 1653–1689, 2023.

[9] J. D. Stark, J. Ridley, M. Martin, and A. Hines, "Sea ice concentration and motion assimilation in a sea ice-ocean model", Journal of Geophysical Research: Oceans, vol. 113, no. C5, 2008.

[10] S. Fritzner, R. Graversen, K. H. Christensen, P. Rostosky, and K. Wang, "Impact of assimilating sea ice concentration, sea ice thickness and snow depth in a coupled ocean–sea ice modelling system", The Cryosphere, vol. 13, pp. 491–509, 2019.

[11] E. Blanchard-Wrigglesworth, R. I. Cullather, W. Wang, J. Zhang, and C. M. Bitz, "Model forecast skill and sensitivity to initial conditions in the seasonal sea ice outlook," Geophysical Research Letters, vol. 42, no. 19, pp. 8042–8048, 2015.

[12] Y. Ren and X. Li, "Predicting daily arctic sea ice concentration in the melt season based on a deep fully convolution network model," in 2021 IEEE International Geoscience and Remote Sensing Symposium IGARSS, pp. 5540–5543, 2021.

[13] Q. Yan and W. Huang, "Sea Ice Sensing From GNSS-R Data Using Convolutional Neural Networks," IEEE Geoscience and Remote Sensing Letters, vol. 15, no. 10, pp. 1510-1514, 2018.

[14] Q. Liu, R. Zhang, Y. Wang, H. Yan, and M. Hong, "Daily prediction of the arctic sea ice concentration using reanalysis data based on a convolutional lstm network," Journal of Marine Science and Engineering, vol. 9, no. 3, 2021.

[15] L. Hoffman, M. R. Mazloff, S. T. Gille, D. Giglio, C. M. Bitz, P. Heimbach, and K. Matsuyoshi, "Machine learning for daily forecasts of arctic sea-ice motion: an attribution assessment of model predictive skill," Artificial Intelligence for the Earth Systems, pp. 1 – 45, 2023.

[16] Z. I. Petrou and Y. Tian, "Prediction of sea ice motion with convolutional long short-term memory networks," IEEE Transactions on Geoscience and Remote Sensing, vol. 57, no. 9, pp. 6865–6876, 2019.

[17] G. E. Karniadakis, I. G. Kevrekidis, L. Lu, P. Perdikaris, S. Wang, and L. Yang, "Physics-informed machine learning," Nature Reviews Physics, vol. 3, pp. 422–440.2021.

[18] P. R. Holland and R. Kwok, "Wind-driven trends in antarctic sea-ice drift," Nature Geoscience, vol. 5, pp. 872–875, 2012.

[19] W. D. Hibler, "A dynamic thermodynamic sea ice model," Journal of Physical Oceanography, vol. 9, no. 4, pp. 815 – 846, 1979.

[20] A. S. Thorndike and R. Colony, "Sea ice motion in response to geostrophic winds," Journal of Geophysical Research: Oceans, vol. 87, no. C8, pp. 5845–5852, 1982.

[21] T. R. Andersson, J. S. Hosking, M. Perez-Ortiz, B. Paige, A. Elliott, C. Russell, S. Law, D. C. Jones, J. Wilkinson, T. Phillips, J. Byrne, S. Tietsche, B. B. Sarojini, E. Blanchard-Wrigglesworth, Y. Aksenov, R. Downie, and E. Shuckburgh, "Seasonal arctic sea ice forecasting with probabilistic deep learning," Nature Communications, vol. 12, no. 5124, 2021.

[22] Y. J. Kim, H.-C. Kim, D. Han, S. Lee, and J. Im, "Prediction of monthly arctic sea ice concentrations using satellite and reanalysis data based on convolutional neural networks," The Cryosphere, vol. 14, no. 3, pp. 1083–1104, 2020.

[23] Y. Ren, X. Li, and W. Zhang, "A data-driven deep learning model for weekly sea ice concentration prediction of the pan-arctic during the melting season," IEEE Transactions on Geoscience and Remote Sensing, vol. 60, pp. 1–19, 2022

[24] Y. Koo, and M. Rahnemoonfar, "Multi-task Deep Convolutional Network to Predict Sea Ice Concentration and Drift in the Arctic Ocean," arXiv:2311.00167, 2023.

[25] W. N. Meier, F. Fetterer, A. K. Windnagel, and J. S. Stewart, "Noaa/nsidc climate data record of passive microwave sea ice concentration, version 4," 2021.

[26] M. Tschudi, J. S. Meier, W. N. Stewart, C. Fowler, and J. Maslanik, "Polar pathfinder daily 25 km ease-grid sea ice motion vectors, version 4," 2019

[27] H. Hersbach, B. Bell, P. Berrisford, S. Hirahara, A. Horanyi, J. Munoz-Sabater, J. Nicolas, C. Peubey, R. Radu, D. Schepers, A. Simmons, C. Soci, S. Abdalla, X. Abellan, G. Balsamo, P. Bechtold, G. Biavati, J. Bidlot, M. Bonavita, G. De Chiara, P. Dahlgren, D. Dee, M. Diamantakis, R. Dragani, J. Flemming, R. Forbes, M. Fuentes, A. Geer, L. Haimberger, S. Healy, R. J. Hogan, E. Holm, M. Janiskova, S. Keeley, P. Laloyaux, P. Lopez, C. Lupu, G. Radnoti, P. de Rosnay, I. Rozum, F. Vamborg, S. Villaume, and J.-N. Thepaut, "The era5 global reanalysis," Quarterly Journal of the Royal Meteorological Society, vol. 146, no. 730, pp. 1999–2049, 2020.